Research Article

Sequencing and Phylogenetic Analysis of GPCR, RPO30, P32 and EEV Glycoprotein Genes of Lumpy Skin Disease Virus Recent Isolates in Egypt

Moustafa A. Zaghloul[1]*, Mohamed F. Azooz[1], Saleh E. Ali[1]*, Heba M. Soliman[1], Maha M. Sayed[1], Mohamed H. Kafafy[2] and Alaa R. Morsy[1]

[1]Central Laboratory for Evaluation of Veterinary Biologics, Agricultural Research Center, Cairo, Egypt; [2]Veterinary Serum and Vaccine Research Institute, Agricultural Research Center, Cairo, Egypt.

Abstract | Lumpy skin disease is an emerging viral illness of ruminants that is highly contagious and economically damaging. The goal of this study is to perform sequencing and phylogenetic analysis of GPCR, RPO30, P32 and EEV glycoprotein genes of Lumpy Skin Disease Virus (LSDV) recent isolates in Egypt, as well as to use artificial intelligence to predict the immunogenic landscape of circulating lumpy skin disease in the Egyptian cattle dairy sector, which will lead to universal blueprints for multiepitope lumpy skin disease vaccine designs. A total of 40 skin nodule samples were collected from clinically affected cattle to detect LSDV using PCR targeting GPCR, RPO30, P32 and EEV glycoprotein genes. The amplified products of samples detected in the skin nodules of cattle were sequenced, and the phylogenetic tree was constructed using crustal omega software. Out of 40 analyzed samples, 25 samples were positive for LSDV by PCR assay. The sequence alignment of the obtained LSDV strain showed high identity to LSD strains from South Africa, Australia, Kenya, Sudan, Ethiopia, Russia, Bangladesh and Iran. Initially, possible T-cell and B-cell epitopes were predicated by manipulating the four antigenic proteins GPCR, RPO30, P32 and EEV. Several bioinformatic methods were employed to find superior epitopes. Fifty-three epitopes passed the three B-cell prediction tools. Twelve promising and top linear B epitopes passed the antigenicity, allergenicity and toxicity tests. Fifty-seven MHC I epitopes were the most promising, while (49) were from MHC II. Thirteen peptides for MHC II were chosen as the best targets for the vaccine. Seventeen MHC I epitopes were the most promising because they were able to bind to the greatest number of MHC Ialleles and passed the antigenicity, allergenicity and toxicity tests. This study shows how important disease surveillance is and how important it is to figure out where the disease came from, how far it spread, how it gets around and how to control it. Overall, the study showed that the novel chimeric LSD-based vaccination can elicit both humoral and cell-mediated immune responses making it a reliable model for future in vivo and in vitro studies for control LSD infection in Egyptian cattle dairy farms.

Received | October 13, 2022; **Accepted** | December 14, 2022; **Published** | January 24, 2023
***Correspondence** | Moustafa A. Zaghloul, Central Laboratory for Evaluation of Veterinary Biologics, Agricultural Research Center, Cairo, Egypt; **Email:** moustafazaghlool@gmail.com
Citation | Zaghloul, M.A., M.F. Azooz, S.E. Ali, H.M. Soliman, M.M. Sayed, M.H. Kafafy and A.R. Morsy. 2023. Sequencing and phylogenetic analysis of GPCR, RPO30, P32 and EEV glycoprotein genes of lumpy skin disease virus recent isolates in Egypt. Journal of Virological Sciences, 11(1): 1-11.
DOI | https://dx.doi.org/10.17582/journal.jvs/2023/11.1.1.11
Keywords | LSDV, PCR, B Epitopes, T Epitopes, Bioinformatics

Introduction

Lumpy skin disease (LSD) is one of the major health issues affecting most African countries livestock industries. It is a severe variant that is both apparent and marked by a rapid rise in temperature (Tasioudi *et al*., 2016; Sprygin *et al*., 2018a). The disease causes significant economic losses to livestock farmers due to milk loss, hide damage, and reproductive issues such as abortion and infertility in affected animals. LSD is a viral disease of cattle, caused by lumpy skin disease virus (LSDV) within the genus Capripoxvirus, family Poxviridae. The genus Capripoxvirus also comprises goatpox virus (GTPV) and sheeppox virus (SPPV); it is Double-stranded DNA and makes up its approximately 150,000 base pairs (bp) long genome (Tulman *et al*., 2001). These viruses cause the majority of economically significant diseases in domestic ruminants in Africa and Asia (CFSPH, 2008).

All breeds and ages of cattle were mechanically exposed to the LSDV through haematophagous arthropod vectors such as stable flies and mosquitoes (Agianniotaki *et al*., 2017; Lu *et al*., 2020). LSDV is primarily found in southern, central, eastern, and western Africa (Lefèvre and Gourreau, 2010). Its presence in the North Sahara desert and outside of Africa was confirmed for the first time in Egypt between 1988 and 1989 and was reported again in Egypt in 2006, 2011 and 2014 (Elhaig *et al*., 2017). LSD incidence has also been reported in the Middle East, Europe and West Asia (Sameea *et al*., 2016). The disease spread to south-east Europe, the Balkans and the Caucasus in 2015 and 2016 (OIE, 2017).

When LSD first appeared in Egypt in 1988, it was regarded as merely another example of an exotic disease that usually entered the country through the importation of live animals. Within a few short years, it had evolved into a national crisis, with the disease being declared enzootic. The disease then resurfaced in the summer of 1989 (Davies, 1991). LSDV struck most Egyptian governorates in 2006 (Awadin *et al*., 2011) and it reappeared in 2011 and 2014 (Amin *et al*., 2015).

LSD symptoms in cattle range from slight to severe, with fever, multiple skin nodules covering the neck, back, perineum, tail, limbs and genital organs and mucous membranes. The lesions may also involve subcutaneous tissues, musculature and internal organs. Affected animals also show lameness, emaciation and a decrease in milk production. Edemas of the limbs and brisket, as well as lymphadenitis, are extremely common and affected animals may die. Furthermore, pneumonia is a frequent complication in animals with mouth and respiratory tract lesions (Tageldin *et al*., 2014).

Indeed to control and prevent infections brought on by a variety of pathogens; vaccines are widely produced and utilized worldwide. Although they are expensive and time-consuming, conventional methods are mostly used for vaccine development and production. It is now possible to design and develop novel peptide-based "subunit vaccines" comprised of the antigenic protein portions from a target pathogen, in contrast to conventional vaccine development methods. This is made possible by cutting-edge research and technology, as well as the availability of information about the genome and proteome of almost all viruses and organisms.

The fact that toxic and immunogenic components of an antigen can be eliminated during a vaccine design study, so that the vaccine can be used safely in animals is a major advantage of subunit vaccines. As a result, bioinformatics and immunoinformatics methods that can be used to create safe, effective, inexpensive and novel subunit vaccines have been developed.

The goal of this study is to perform sequencing and phylogenetic analysis of G protein-coupled receptor (GPCR), RNA polymerase 30 kDa subunit (RPO30), P32, and extracellular enveloped virus (EEV) glycoprotein genes of LSDV recently isolated in Egypt, as well as to use artificial intelligence to predict the immunogenic landscape of circulating LSD in the Egyptian dairy cattle sector, which will lead to universal blueprints for multi epitope LSD vaccine designs.

Materials and Methods

Area of study

Samples were collected from nearby livestock reared in 2 governorates; Menofia governorate in the northern part of Egypt beside the Nile Delta, to the South of Gharbia governorate and to the north of Cairo. The 2nd governorate was Sharqia governorate that is the third maximum populous of the governorates of

Egypt and located in the northern part of the country.

Study period, location, animal examination and sample collection

Skin biopsies made up of the epidermis, dermis and subcutis of the nodular skin lesions were taken from local cattle raised in Menofia and Sharqia governorates between the 2020 and 2022. The animal study included physical indicators like temperature, superficial lymph node and skin lesions (Sohier *et al.*, 2019). Symptoms of biphasic fever (40°C - 41.5°C), in appetence, depression, salivation and ocular-nasal discharge were observed in cattle. The prescapular and precrural superficial lymph nodes, showed significant enlargement. The samples were taken in sterile 15 ml tubes, transported to the laboratory and kept at -70°C until used.

Sample preparation

Tissue samples were prepared using the protocols indicated by OIE (2010). Using a sterile mortar each cow's nodules were minced and suspended in sterile phosphate-buffered saline (PBS) containing 10% Gentamycine antibiotic solution. Tissue homogenates were centrifuged for 10 minutes at 1500 xg under 4°C. Clear supernatants were frozen at -70°C until used.

Virus isolation

The field virus was isolated from infected animals using 11-days old specific pathogen-free embryonated chicken eggs (SPF-ECEs) via chorioallantoic membrane (CAM) route as described by Van Rooyen (1969). Briefly, 200 µl of each tissue homogenate's supernatant fluid was injected into five ECEs, incubated for five days at 37°C and examined daily for typical pock's lesions on infected CAMs. After being suspended in PBS, the infected CAMs were minced with sterile pestles and centrifuged for 10 minutes at 1500 xg in a cooling centrifuge. The CAMs' supernatant fluid was kept at -70°C for further investigations.

Polymerase chain reaction

Following the manufacturer's instructions, DNA was extracted from samples using the QIAamp DNA Mini kit (Qiagen, Germany, GmbH).

Using the following primers pair, as shown in Table 1, a specific PCR assay that targeted the GPCR, RPO30, P32 and EEV glycoprotein genes was performed used to confirm the presence of LSDV. The reaction was set up in Applied Biosystems 2720 thermal cycler with a final volume of 25 µl. It contained 1 µl of each primer with a concentration of 20 pmol, 12.5 µl of Emerald Amp Max PCR Master Mix (Takara, Japan), 6 µl of DNA template and 4.5 µl of water. PCR products were analyzed on 1.5% agarose gel electrophoresis (AppliChem, Germany, GmbH) in 1 each gel slot contained 15 µl of the products for gel analysis. The 570 bp GelPilot 100 bp DNA Ladder from Qiagen, Germany, GmbH was used to confirm LSDV-positive samples. The gel was photographed with an Alpha Innotech gel documentation system from Biometra and computer software was used to process the data.

Phylogenetics and gene sequence analyses of GPCR, RPO30, P32 and EEV glycoprotein genes of lumpy skin disease virus

A total of 19 (GPCR, RPO30, P32 and EEV genes) of LSDV isolates were retrieved from the GenBank database. The strains were selected to represent the different virus genotypes, different countries worldwide, and different years. A BLAST® (Basic Local Alignment Search Tool) https:/ blast.ncbi.nlm.nih.gov/Blast.cgi analysis to obtain the DNA sequences.

Table 1: *Primers pairs, amplicon size used in specific PCR assay that targeted the GPCR, RPO30, P32 and EEV glycoprotein genes was used to confirm the presence of LSDV.*

Primer name	Sequence (5' → 3')	Amplicon size	Reference
-F EEV gene	5'-ATGGGAATAGTATCTGTTGTATACG -3'	958 bp	Chibssa *et al.* (2021)
-R EEV gene	5'-CGAACCCCTATTTACTTGAGAA -3'		
-F GPCR gene	5'-TTAAGTAAAGCATAACTCCAACAAAAAATG-3'	6961 – 8119 bp	Le Goff *et al.* (2009)
-R GPCR gene	5'-TTTTTTTATTTTTTATCCAATGCTAATACT-3'		
-F RPO30 gene	5'-CAGCTGTTTGTTTACATTTGATTTTT-3'	554 bp	Gelaye *et al.* (2015)
-R RPO30 gene	5'-TCGTATAGAAACAAGCCTTTAATAGA-3'		
-F P32 gene	5'-GACGATAATCTAATTACATATG-3'	587 bp	(Ireland and Binepal, 1998)
-R P32 gene	5'-ATGGCAGATATCCCATTATATGTTA-3'		

The QIAquick PCR Product extraction kit was utilized for product purification (Valencia, Qiagen) for the sequence reaction. The Bigdye Terminator V3.1 cycle sequencing kit from Perkin-Elmer was used and the Centrisep spin column was used to purify the product. Sequence fragments corresponding genes (your study) were edited and trimmed from the international sequences using Editseq program of Laser gene software, version 3.18 (DNAStar, Madison, WI). Multiple sequence alignment GPCR, RPO30, P32 and EEV genes and their corresponding amino acid sequences were generated and identification of mutation sites was performed using Muscle3.8.31 algorithm. The phylogenetic trees were constructed based on GPCR, RPO30, P32 and EEV genes. Phylogenetic analysis was performed using the maximum likelihood method of TreeDyn 198.3 software.

Immuno-informatics and machine learning based approaches linear B cell epitope prediction

Epitopes for the B cell receptor (BCR) will be predicted using a variety of techniques. In this study, linear B cell epitopes were predicted using SVMTriP (http://sysbio.unl.edu/SVMTriP/resultphp?jobid=6364a604dedd15.25614780). Artificial neural network-based B-cell epitope prediction server (ABCpred) was initially used to predict epitopes for 14-mers, using a default recurrent neural network threshold of 0.51 (http://www.imtech.res.in/raghava/abcpred/). Finally, a novel approach for predicting linear B-cell epitopes utilizing kernel approaches, the BCPreds server, will be used (https://webs.iiitd.edu.in/raghava/ bcepred/ bcepred_submission.html).

MHC-I and MHC-II binding epitope prediction

Using artificial neural networks, NetMHCpan 4.0 (http://www.cbs.dtu.dk/services/NetMHCpan/) was utilized to forecast the binding of peptides (8–11 amino acids) in linear form to MHC class I groove (ANNs). The percentile rank threshold for peptide MHC-I binding affinity will be settled at 0.5% for strong binders and 2% for weak binders. RANKPEP" (http://imed.med.ucm.es/Tools/rankpep.html) predicts MHC-II binding epitopes which are based on their Position Specific Scoring Matrices (PSSMs) ranking for all possible peptides. Additionally, the IEDB MHC-I and MHC-II binding prediction tools (http://tools.iedb.org/mhci/and http://tools.iedb.org/mhcii/) will be utilized to forecast the capacity of peptides in linear form for interacting with MHC-I and MHC-II grooves. To obtain percentile ranks for expected peptide-MHC complexes, the EDB-suggested approach was used. Additionally, each protein sequence in this study was examined independently.

Antigenicity, allergenicity and toxicity analysis

Each CTL, CD4 T cell and B-cell epitope was predicted for antigenicity, allergenicity, and toxicity. The antigenicity of peptides was predicted using the web-servers VaxiJen v2.0 (http://www.ddg-pharmfac.net/vaxijen/VaxiJen /VaxiJ en.html). An AllerTOP v2.0 web server was used to calculate the potential allergenicity of the chosen epitopes. ToxinPred, a web server, was used to calculate the potential toxicity of the chosen epitopes for the host (https://webs.iiitd.edu.in/raghava/toxinpred/).

Results and Discussion

The most common symptoms of cattle infected with LSD were pyrexia, salivation, nasal and ocular discharges, decreased milk yield, enlargement of prefemoral and prescapular lymph nodes and skin nodules covering the head, neck, trunk, perineum, teats and sometimes the entire body. The skin nodules had the appearance of deep scabs and ulcerations and affected the epidermis, dermis, sub cutis and muscles (Figure 1).

Figure 1: *Lumpy skin disease infected animal shows cutaneous nodules covering the entire body.*

A specific PCR assay that targeted the GPCR, RPO30, P32 and EEV glycoprotein genes was used to confirm the presence of LSDV viral DNA from suspected clinical cases. By using PCR, 25 out of 40 samples analyzed were positive for LSDV. These 25 samples were from the outbreak in 2021.

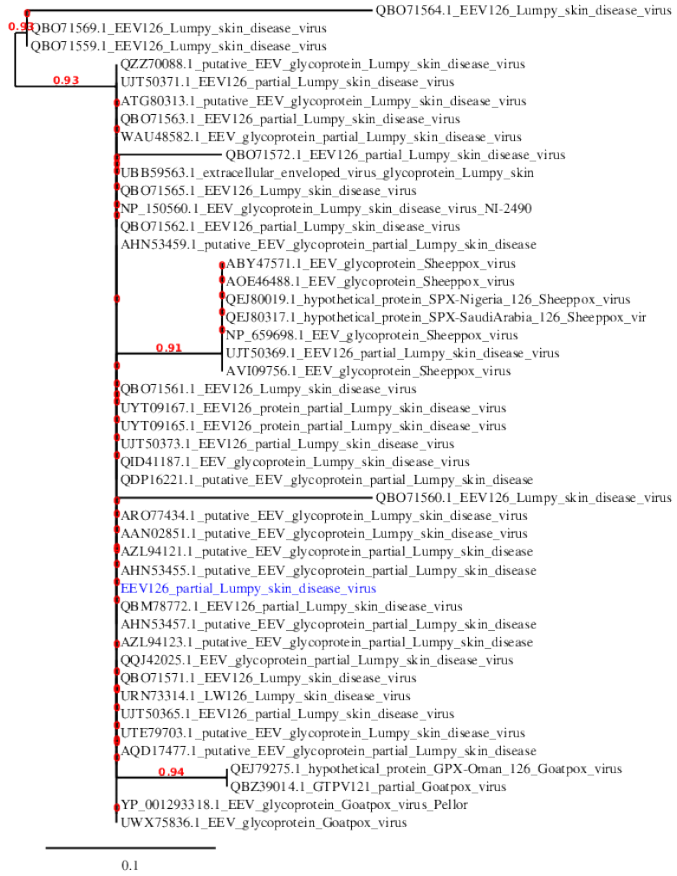

Figure 2: *Maximum likelihood phylogenetic tree of LSDV isolates based on the deduced amino acids sequences of 126 EEV proteins showing the genetic relationship between the Egyptian LSDV isolate (LSDA) obtained in this study and other selected LSDV sequences.*

```
LSDA            LLISYIFFEYKNVIKKMLFKKKGKNQKRTCVRLNSITYSTNSIKSTISESTWSNCSNDTF  600
UJT50365.1      VLLSYIFFEYKNVIKKMLFKKKGKNQKRTCVRLNSITYSTNSIKSTISESTWSNCSNDTF   74
ARO77434.1      VLLSYIFFEYKNVIKKMLFKKKGKNQKRTCVRLNSITYSTNSIKSTISESTWSNCSNDTF   76
UJT50373.1      VLLSYIFFEYKNVIKKMLFKKKGKNQKRTCVRLNSITYSTNSIESTISESTWSNCSNDTF   74
NP_150560.1     VLLSYIFFEYKNVIKKMLFKKKGKNQKRTCVRLNSITYSTNSIESTISESTWSNCSNDTF   76
QBO71565.1      VLLSYIFFEYKNVIKKMLFKKKGKNQKRTCVRLNSVTYSTNSIKSTISESTWSNCSNDTF   76
AHN53459.1      ------------------------------------------------SNCSNDTF      8
AHN53457.1      ------------------------------------------------NCSNDTF       7
ATG80313.1      VLLSYIFFEYKNVIKKMLFKKKGKNQKRTCVRLNSITYSTNSIKSTISESTWSNCSNDTF   76
                                                                 *******

LSDA            VKNEKENVKIVEIKRCDNELIEESNNNVLENGCTTNTGEENLIWDDNNVYDLPPNDSVYD  660
UJT50365.1      VKNEKENVKIVEIKRCDNELIEESNNNVLENGCTTNTGEENLIWDDNNVYDLPPNDSVYD  134
ARO77434.1      VKNEKENVEIVEIKRCDNELIEESNNNVLENGCTTNTGEENLIWDDNNVYDLPPNDSVYD  136
UJT50373.1      VKNEKENVEIVEIKRCDNELIEESNNNVLENGCTTNTGEENLIWDDNNVYDLPPNDSVYD  134
NP_150560.1     VKNEKENVEIVEIKRCDNELIEESNNNVLENGCTTNTGEENLIWDDNNVYDLPPNDSVYD  136
QBO71565.1      VKNEKENVEIVEIKRCDNELIEESNNNVLENGCTTNTGEENLIWDDNNVYDLPPNDSVYD  136
AHN53459.1      VKNEKENVEIVEIKRCDNELIEESNNNVLENGCTTNTGEENLIWDDNNVYDLPPNDSVYD   68
AHN53457.1      VKNEKENVEIVEIKRCDNELIEESNNNVLENGCTTNTGEENLIWDDNNVYDLPPNDSVYD   67
ATG80313.1      VKNEKENVEIVEIKRCDNELIEESNNNVLENGCTTNTGEENLIWDDNNVYDLPPNDSVYD  136
                ********:**************************************************

LSDA            LPPNDLSCNNDCVYTLPDDNVSNIEEKITKLMHKNNSESNYYNCCKFHEKNIVDSVFYHN  720
UJT50365.1      LPPNDLSCNNDCVYTLPDDNVSNIEEKITKLMHKNNSESNYYNCC---------------  179
ARO77434.1      LPPNDLSCNNDCVYTLPDDNVSNIEEKITKLIHKNNSESNYYNCC---------------  181
UJT50373.1      LPPNDLSCNNDCVYTLPDDNVSNIEEKITKLMHKNNSESNYYNCC---------------  179
NP_150560.1     LPPNDLSCNNDCVYTLPDDNVSNIEEKITKLMHKNNSESNYYNCC---------------  181
QBO71565.1      LPPNDLSCNNDCVYTLPDDNVSNIEEKITKLMHKNNSESNYYNCC---------------  181
AHN53459.1      LPPNDLSCNNDCVYTLPDDNVSNIEEKITKLMHKNNSESNYYNCC---------------  113
AHN53457.1      LPPNDLSCNNDCVYTLPDDNVSNIEEKITKLMHKNNSESNYYNCC---------------  112
ATG80313.1      LPPNDLSCNNDCVYTLPDDNVSNIEEKITKLMHKNNSESNYYNCC---------------  181
                *******************************:*************
```

Figure 3: *Alignment of deduced amino acids of the EEV genes. The Egyptian LSDA isolate was aligned with representative LSDV sequences retrieved from GenBank.*

A maximum likelihood phylogenetic tree of LSDV isolate (LSDA) was constructed based on the deduced amino acids sequences of 126 amino acids of EEV proteins (Figure 2). The sequenced LSDV isolate was clustered with other LSDV from Egypt and different countries. The field LSDV isolate was closely related to other LSDV sequences from Russia, Bangladesh, South Africa, Israel and Kenya. The sequenced sample outbreak samples showed amino acids sequence identities of 99.01% with AZL94123.1 (outbreak in 2015), 99.07% with QQJ42025.1 (outbreak in 2019), 99.11% with AHN53457.1 (outbreak in 2012) and 98.18% with ATG80313.1 (outbreak in 2012). The multiple sequence alignment of the 126 EEV amino acids showed amino acids substitutions between the fields isolate and other representative LSDV sequences retrieved from GenBank (Figure 3) at positions: V541 L, E609 K and E584 K.

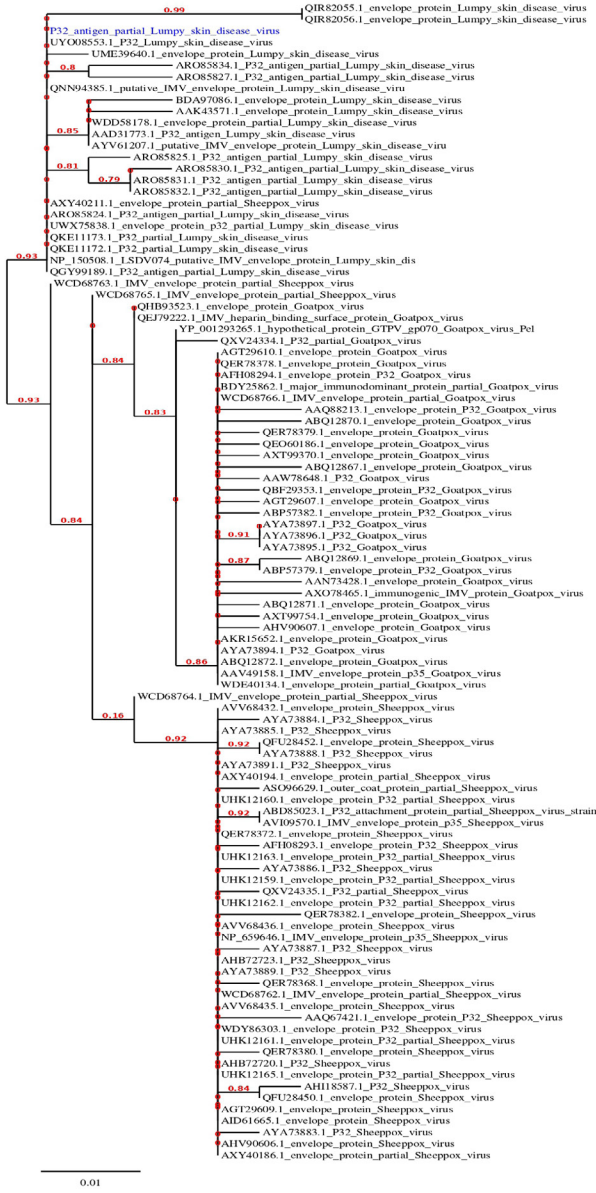

Figure 4: *Maximum likelihood phylogenetic tree of LSDA isolate based on the deduced amino acids sequences of P32 protein showing genetic relationship between the Egyptian LSDA isolate obtained in this study and other selected LSDVs.*

Maximum likelihood phylogenetic tree of LSDV isolate (LSDA) based on the deduced amino acids sequences of P32 protein (Figure 4) showed that the Egyptian LSDA isolate clustered was closely related to other LSDV sequences from Egypt (Beni-Suef), Australia, India and Iran. For the P32 protein, the amino acids sequence homology between LSDV isolate from Egypt and LSDV field strains from other countries was in the range of 99.58%–100% and the highest homology was found with Iran strains. The multiple sequence alignment of the P32 protein showed amino acids sequence substitutions between the field isolates and other representative LSDV sequences retrieved from GenBank (Figure 5) at positions: N113 D, K112 E and K132 E.

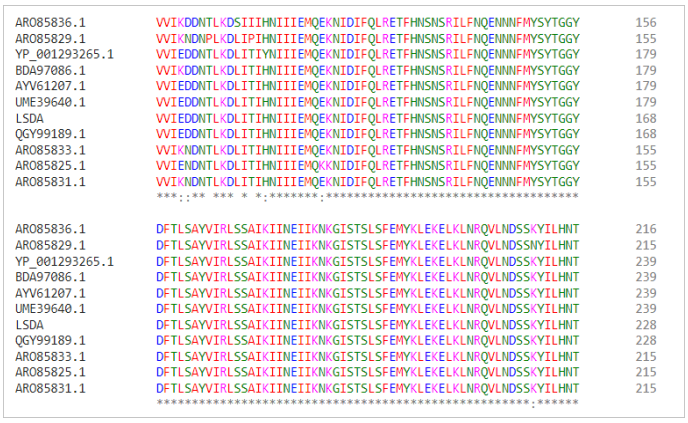

Figure 5: *Multiple sequence alignments of deduced amino acids of the P32 gene of LSDV. The Egyptian LSDA isolate was aligned with representative LSDV sequences retrieved from GenBank.*

As shown in Figure 6 maximum likelihood phylogenetic tree of LSDV isolate (LSDA) based on the deduced amino acids sequence of G-protein-coupled chemokine receptor (GPCR) Protein clarified that the Egyptian LSDA isolate was clustered with other LSDV sequences from Egypt (Sharkia and Dakahlia), Ethiopia, Syria, South Africa and Turkey. For GPCR protein, the amino acids sequence homology between LSDA isolate from Egypt and LSDV field strains from other countries was in the range of 99.65%–100% and the highest homology was found with Turkey strains.

As shown in Figure 7 the multiple sequence alignment of the GPCR protein showed amino acids sequence substitutions between the field isolates and other representative LSDV sequences retrieved from GenBank at positions: K360 N, V250 I.

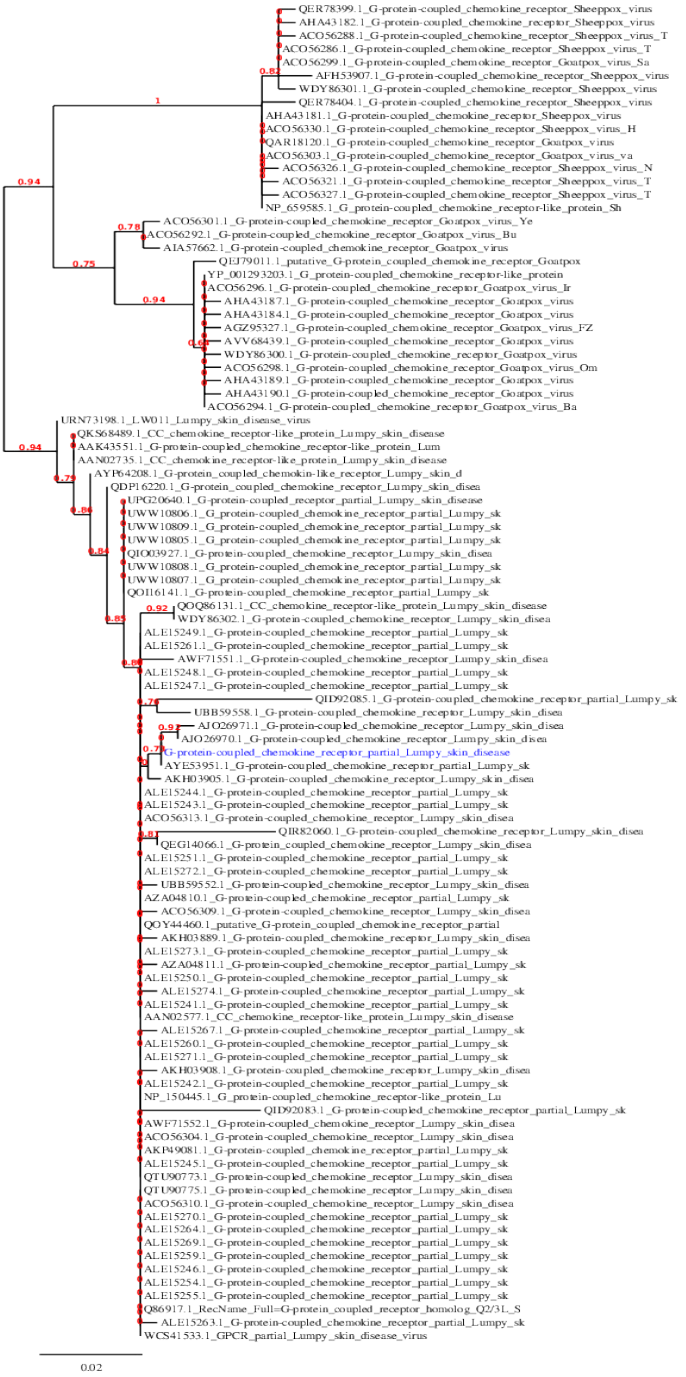

Figure 6: *Maximum likelihood phylogenetic tree of LSDA isolate based on the deduced amino acids sequences of G-protein-coupled receptor (GPCR) protein showing genetic relationship between the Egyptian LSDA isolate obtained in this study and other selected LSDVs.*

As shown in Figure 8 maximum likelihood phylogenetic tree of LSDV isolate (LSDA) based on the deduced amino acids sequence of RNA polymerase subunit 30 kD (RPO30) protein clarified that the Egyptian LSDA isolate was closely related to other LSDV sequences from Sudan, Kenya, Mongolia, Russia and India. For RPO30 protein, the amino acids sequence homology between LSDA isolate from Egypt and LSDV field strains from other

countries was in the range of 98.73% – 100% and the highest homology was found with Sudan strains.

Figure 7: *Multiple sequence alignments of deduced amino acids of the G-protein coupled chemokine receptor (GPCR) gene of LSDA. The Egyptian LSDA isolate was aligned with representative LSDV sequences retrieved from GenBank.*

The multiple sequence alignment of the RPO30 protein (Figure 9) showed amino acids sequence substitutions between the field isolates and other representative LSDV sequences retrieved from GenBank at positions: M60 I, L84 S, G158 E, W159 C and F183 S.

Fifty-three epitopes passed the three B-cell prediction tools BCPreds, SVMTriP and ABCpred (Tables 6, 7 and 8, respectively). The most promising and top linear B epitopes passed the antigenicity, allergenicity and toxicity tests are illustrated in Table 10. Artificial neural networks, NetMHCpan 4.0 and IEDB MHC-I binding prediction tools were applied to forecast the binding of peptides (8-11 amino acids) in linear form to MHC class I groove (ANNs). The percentile rank threshold for peptide-MHC-I binding affinity was settled at 0.5% for strong binders and 2% for weak binders. The results of the prediction of MHC-I binding epitopes in LSDV proteins were illustrated in (Table 9). Fifty seven peptides were predicted to interact with different MHC class I alleles.

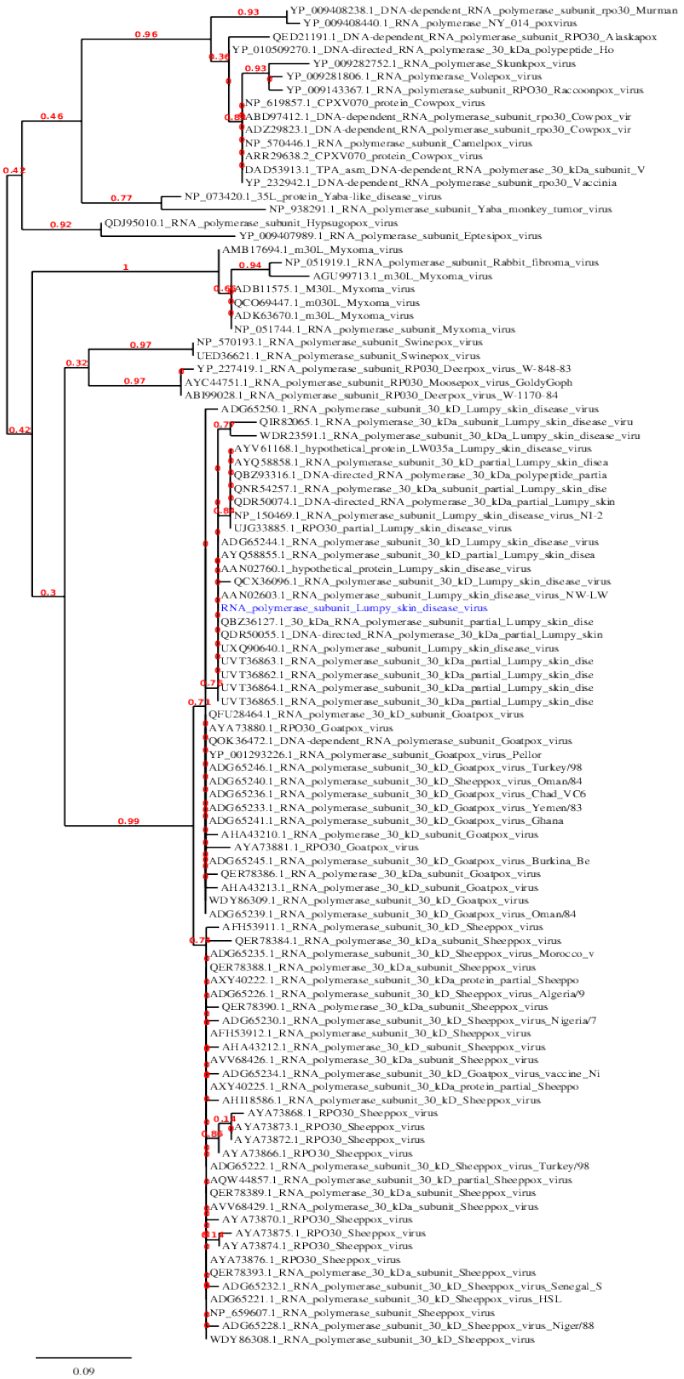

Figure 8: *Maximum likelihood phylogenetic tree of LSDA isolate based on the deduced amino acids sequences of RNA polymerase subunit 30 kD subunit (RPO30) protein showing genetic relationship between the Egyptian LSDA isolate obtained in this study and other selected LSDV, GTPV and SPPV strains.*

RANKPEP (http://imed.med.ucm.es/Tools/rankpep.html) server predicts MHC-II binding epitopes which are based on their Position Specific Scoring Matrices (PSSMs) ranking for all possible peptides. The results of the prediction of MHC-I binding epitopes in LSDV proteins were illustrated in Tables 2, 3, 4 and 5. Peptides were predicted to interact with different MHC-II alleles.

Figure 9: *Multiple sequence alignments of deduced amino acids of RNA polymerase 30 kD subunit (RPO30) protein of LSDV. The Egyptian LSDA isolate was aligned with representative LSDV sequences retrieved from GenBank.*

Table 2: *MHC-II binding epitope prediction in EEV protein. The position specific scoring matrix (PSSM) specific binding threshold reported by RANKPEP software is obtained by scoring all the peptide sequences included in the alignment from which a profile is derived and defined as the score value that includes 85% of the peptides within the set.*

Position	MHC class II -Allele	Epitope	Score
158	HLA-DR51 (DRB5*0101)	FNMKNKIFR	22.559
504		FNKATKNKK	19.779
559		FKKKGKNQK	19.753
428		FRFLISLKK	18.16
1679		YSKNIYEIR	17.895
207	HLA-DR5	RYLKIYRYD	25.567
1010		HYHVVNHKR	20.708
1192		KYLFVNILF	19.958
1066		MYHYYNLTK	19.864
52		QIVVMIHLK	19.199
1207	HLA-DR4 (DRB1*0404)	VYMFFIIVF	16.225
1101		FITFFHFCI	15.215
954		KYFIFHVKI	15.215
690		KLMHKNNSE	14.531
1045		QLIHYHNVF	14.522

LSD is a transboundary viral disease of cattle and buffaloes transmitted by blood-feeding vectors and causes high morbidity and low to moderate mortality. In areas of mixed crop-livestock production, LSD is endemic and pervasive. At the level of the individual animal and the entire herd, the LSD seroprevalence is high. The availability of water bodies, adult age, and contact with other animals are all significant risk factors for LSD. Priority places for conservation efforts could include those having access to rivers, lakes, ponds, dams, irrigated land, swamps and cow herds with a high proportion of LSD adult animals (Wassie *et al.*, 2018).

Table 3: *MHC class II binding epitope prediction in P32 protein. The position specific scoring matrix (PSSM) specific binding threshold reported by RANKPEP software is obtained by scoring all the peptide sequences included in the alignment from which a profile is derived and defined as the score value that includes 85% of the peptides within the set.*

Position	MHC class II -Allele	Epitope	Score
583	HLA-DR51 (DRB5*0101)	FSFNIVQSR	19.855
307		YVMLFVQKR	17.919
406		YRLPKTKLK	17.492
893		FDKYLVLSI	17.285
649		YTSQYVFVK	17.24
625	HLA-DR5	YFYQFKFNV	19.399
20		YKKVDTVKD	17.551
444		YFTILSICQ	16.691
773		YCYIFCVII	15.341
559		IKRFNNNTH	15.011
239	HLA-DR11 (DRB1*1101)	MKLVAKFQM	16.161
501		YMGKGRKIR	14.912
400		YPHMLDYRL	14.177
713		YYFYGRRSN	13.346

Table 4: *MHC-II binding epitope prediction in RNA polymerase 30 kD subunit (RPO30) protein. The position specific scoring matrix (PSSM)-specific binding threshold reported by RANKPEP software is obtained by scoring all the peptide sequences included in the alignment from which a profile is derived, and defined as the score value that includes 85% of the peptides within the set.*

Position	MHC class II -Allele	Epitope	Score
25	HLA-DR51 (DRB5*0101)	YKYVKEKSK	21.39
27		YVKEKSKVK	17.575
37	HLA-DR4 (DRB1*0404)	ILKWATDKA	16.53
8		SYSDNTTPT	13.042
171		TRAADEPPL	10.173
101		CDLIRTTNG	8.272
50	HLA-DR4 (DRB1*0402)	IRNIINTKS	18.19
37		ILKWATDKA	17.24

In the current study, the suspected diseased animals showed typical LSD clinical signs such as generalized nodular skin disease, sharp drop in milk production and infertility. Based on the deduced amino acid

sequences of the 126 EEV Protein, a maximum likelihood phylogenetic tree of the LSDV isolate (LSDA) was constructed.

Table 5: *MHC-II binding epitope prediction in GPCR protein. The position specific scoring matrix (PSSM) specific binding threshold reported by RANKPEP software is obtained by scoring all the peptide sequences included in the alignment from which a profile is derived and defined as the score value that includes 85% of the peptides within the set.*

Position	MHC class II - Allele	Epitope	Score
958	HLA-DR4 (DRB1*0401)	YFKNITNKE	17.416
566		WWFGLSQLL	16.998
786		YYKFWTDYF	16.687
1225		SVSINTHQC	15.252
1022		LFYQSTNLC	14.66
	HLA-DR5		
957		KYFKNITNK	27.561
1237		AIVKTNKVK	23.49
1158		KYVYFKIYK	23.207
1777		LYYKTHKLV	21.187
270		YYKILNTLK	19.147
	HLA-DR12 (DRB1*1201)		
2090		YYTWLRYLY	24.963

Table 6: *Predicted Linear B Epitopes predicted from LSDV Proteins using BCPRED server.*

LSDV protein	Position	Epitope
EEV 126	16	KCYLKKKGKIK
	131	MTMFQTRKK
	237	LYVSNQQK
	249	GYLSYKKSS
	267	ISIQHSQ
	276	ALHEKQKA
P32		
	24	DTVKDFNKSD
	35	NFFFKDK
	51	LIWEKVEKSGG
	75	ALCTKEAK
	98	ADIKNSEN
RPO30		
	1	MDDNTNSYSDNT
	25	YKYVKEKSKV
	39	KWATDKA
	72	GIEYSKDSKNK
	102	DLTRTTNGTE
GPCR		
	11	ATMYNSSN
	29	STISTNQ
	275	NTLKTSQTKNK

This sequenced LSDA grouped together with other LSDVs from Egypt and other countries. The other LSDV sequences from Russia, Bangladesh, South Africa and Kenya were closely related to the field LSDV isolate. The sample LSDA shared amino acid sequence identities of 99.01% with AZL94123 (2015 outbreak), 99.07% with QQJ42025 (2019 outbreak), 99.11% with AHN53457 (2012) outbreak and 98.18% with ATG80313 (2012) outbreak. The EEV126 protein multiple sequence alignments revealed amino acid substitutions of: E 609 K, V 541 L and E584 K.

Table 7: *Predicted Linear B Epitopes predicted from LSDV Proteins using SVMTriP server.*

Position	LSDV protein	Linear B Epitope	Score
1540-1559	EEV	LCINLVIFSSMFETLSS-	1.000
44-63	126	GNV	0.960
782-801		PLTQKVLGQIVVMI-	0.956
126-145		HLKMKK	0.946
		SFSKALICIKSAKKVG-	
108-127	RPO30	WLSL	1.000
		FIHYRMTMFQTRK-	
		KLSCTKI	
107-127	P32		1.000
		TNGTEKEILRYILFGIK-	0.951
		CVQ	0.927
175-194	GPCR	VGREISDVVPELKSDN-	1.000
		DIFY	
1669-1688		HMLDYRLPKTKLKIKV-	0.864
		FLPV	
		VYEYIKLLFSLN-	
		NILELLLK	
		FITLMSIDRYLAVVH-	
		PVKSM	
		KNIVEYKVISPKLV-	
		VSTPSS	

A better understanding of the epidemiology, origin and variation of vaccine strains is made possible by the molecular characterization of circulating strains, which also aids in the formulation of control methods. All field strains clustered together according to the results of the phylogenetic analysis using the P32 and fusion gene; however, the vaccine strains remained separate. This obtained result is in agreement with the findings of Manic *et al.* (2019). The results of Sudhakar *et al.* (2020) are supported by the phylogenetic analysis of gene P32, which revealed that P32 of LSDA is genetically more similar to field isolates of LSDV from Egypt, Saudi Arabia and China than to the fusion gene discovered nearby in Kenya, Nigeria, Egypt and Greece.

Table 8: *Predicted Linear B Epitopes predicted from LSDV Proteins using ABCpred Prediction Server the predicted B cell epitopes are ranked according to their score obtained by trained recurrent neural network. Higher score of the peptide means the higher probability to be an epitope. All the peptides shown here are above the threshold value chosen.*

Start position	LSDV protein	Linear B epitope	Score
153	RPO30	NLPCPECKSKNTIP	0.85
145		FNVLDKKYNLPCPE	0.82
107		TNGTEKEILRYILF	0.80
12		NTTPTYQDIEDIIY	0.79
	EEV126		
122		TTIVFIHYRMTMFQ	0.91
386		LCLYITGQCFKHRG	0.89
579		STNSIKSTISESTW	0.87
1151		RPLPHLFCFDTYKC	0.87
668		CNNDCVYTLPDDNV	0.86
321		IHYIRKYLVKLYIC	0.86
1109		IQKIYMKSEAFCFS	0.86
	P32		
706		FIFYNFVYYFYGRR	0.89
169		DFTLSAYVIRLSSA	0.89
468		RIKKQYILKSHSKR	0.88
392		TQGDMILPYPHMLD	0.88
864		VNFFIKYIIVTFFW	0.87
822		RKIFCKIFNTSFFY	0.83
628		QFKFNVVGKRIKTQ	0.83
	GPCR		
1474		KNNTEQITIKNTIF	0.94
1178		MTIRYSIYFFCFIK	093
820		TGYVFAFDTVFNFR	0.92
1374		NCSSYSGNITATII	0.92
515		LNNGVEIVCVNLKL	0.90
34		NQNNVTTPSTYENT	0.90

Based on the deduced amino acid sequences of the P32 protein, a maximum likelihood phylogenetic tree of the LSDV isolate (LSDA) showed that the Egyptian LSDA isolate clustered with other LSDV sequences from Egypt (Beni-Suef), Australia, India and Iran. For the P32 protein, the amino acid sequence homology between the LSDV isolate from Egypt and field strains from other nations was between 99.58 and 100 percent, with Iran strains having the highest homology. The P32 protein multiple sequence alignments revealed amino acid substitutions at K112 E, N 113 D and K132E.

Based on the deduced amino acid sequences of GPCR protein, phylogenetic analyses of the LSDA isolate showed that the isolate is related to other LSDV sequences from Egypt (Sharkia and Dakahlia), Ethiopia, Syria, South Africa and Turkey.

Table 9: *MHC-I binding Epitope prediction in LSDV proteins using artificial neural networks, NetMHCpan 4.0* (http://www.cbs.dtu.dk/services/NetMHCpan/) *was utilized to forecast the binding of peptides (9 amino acids) in linear form to MHC class I groove (ANNs). The percentile rank threshold for peptide-MHC-I binding affinity was settled at 0.5% for strong binders and 2% for weak binders.*

LSDV protein	Epitope	Corresponding BOLA Allele	Percentile rank
RPO30			
	NVLDKKYNL	BoLA-T2c	0.07
	KKNFKPPKF	BoLA-D18.4	0.03
	KSKVKEILK	BoLA-T2a	0.14
	IIYKYVKEK	BoLA-T2a	0.22
	VQKNVEFNI	BoLA-HD6	0.21
EEV			
	HVLDLIQSL	BoLA-T2c	0.01
	AQKFRVKLL	BoLA-HD6	0.02
	RQRLFTTCL	BoLA-HD6	0.02
	YKKKSSISF	BoLA-D18.4	0.01
	KMKKKMRLL	BoLA-HD6	0.03
	GKIKKEHVL	BoLA-D18.4	0.01
	IQIDKILIH	BoLA-D18.4	0.02
	LIQQIVNPL	BoLA-T2c	0.07
	KKSSISFSY	BoLA-D18.4	0.02
	YIRKYLVKL	BoLA-T2c	0.1
	TMFQTRKKL	BoLA-T2c	0.1
	NLKKVIITF	BoLA-T2c	0.11
	NTIMKNMTL	BoLA-T2c	0.12
	YKIHYIRKY	BoLA-D18.4	0.04
GPCR			
	TLSDLIFVL	BoLA-T2c	0.01
	IIQPHIIQL	BoLA-T2c	0.02
	MIIPLTILL	BoLA-T2c	0.03
	TLMSIDRYL	BoLA-T2c	0.04
	NIFGMIIPL	BoLA-T2c	0.04
	KKYMERIVM	BoLA-D18.4	0.01
	VQFQQIKIM	BoLA-D18.4	0.01
	TIACHLHVL	BoLA-T2c	0.05
	TLYSTIFFL	BoLA-T2c	0.05
	SVTVFVSSL	BoLA-T2c	0.05
	DMFLLNLTL	BoLA-T2c	0.05
	DLSTLQFML	BoLA-T2c	0.06
	DVWRDLSTL	BoLA-T2c	0.06
	NVFSGCMAL	BoLA-T2c	0.07
	LLIYTIVSL	BoLA-T2c	0.08
	HLHVLIDTL	BoLA-T2c	0.08
	KQKKYMERI	BoLA-HD6	0.05
	FMRFVVENL	BoLA-T2c	0.1
	KSMPIRTKR	BoLA-T2a	0.05
	TKKVYGITY	BoLA-D18.4	0.03
	VILPLLLQL	BoLA-T2c	0.11
	DSIAKQWSL	BoLA-T2c	0.11
P32			
	VQKRQKVLL	BoLA-HD6	0.01
	EISDVVPEL	BoLA-T2c	0.01
	FLYPHRHTI	BoLA-T2c	0.02
	MILPYPHML	BoLA-T2c	0.02
	NLYDKLISF	BoLA-T2c	0.02
	NILNFQHLL	BoLA-T2c	0.02
	SAYDFHKLK	BoLA-T2a	0.01
	TSLSFEMYK	BoLA-T2a	0.01
	TLSAYVIRL	BoLA-T2c	0.04
	TIHNIIIEM	BoLA-T2c	0.04
	SLNNILELL	BoLA-T2c	0.04
	EMYKLEKEL	BoLA-T2c	0.05
	LKIKKISVY	BoLA-D18.4	0.05
	SLSFEMYKL	BoLA-T2c	0.06
	FVHRGIFYL	BoLA-T2c	0.02
	ISFLSLKKK	BoLA-T2c	0.02

Table 10: *Antigenicity, allergenicity and toxicity of Predicted Linear B Epitopes predicted from LSDV proteins.*

Linear B epitope	Anti-gencity	Allergencity	Toxicity
FIHYRMTMFQTRK-KLSCTKI	0.421	Non allergen	Non toxin
KNIVEYKVISPKLV-VSTPSS	0.6942	Non allergen	Non toxin
NLPCPECKSKNTIP	0.5172	Non allergen	Non toxin
TNGTEKEILRYILF	1.2425	Non allergen	Non toxin
STNSIKSTISESTW	0.7075	Non allergen	Non toxin
DFTLSAYVIRLSSA	1.2581	Non allergen	Non toxin
RIKKQYILKSHSKR	0.5940	Non allergen	Non toxin
TQGDMILPYPHMLD	0.7163	Non allergen	Non toxin
QFKFNVVGKRIKTQ_	1.6211	Non allergen	Non toxin
KNNTEQITIKNTIF	0.5784	Non allergen	Non toxin
TGYVFAFDTVFNFR	0.8683	Non allergen	Non toxin
NQNNVTTPSTYENT	0.6292	Non allergen	Non toxin

For the GPCR protein, the amino acid sequence homology between the LSDA isolate and other field strains was between 99.65 % - 100 %, with the highest homology to Turkey strains those in line with the finding of El-Tholoth and El-Kenawy (2016).

According to Sprygin *et al.* (2018b) some LSDV variants displayed a 12-nucleotide insertion in the GPCR gene, similar to vaccine strains and others displayed a (27) nucleotide deletion in the ORF LSDV 126, similar to the LSDV Neethling vaccine strain. These variants were said to have emerged as a result of recombination between the Neethling vaccine strain and field isolates.

In the present study, the GPCR protein multiple sequence alignments revealed amino acid substitutions at K 360 N, V 250 I and this is in agreement with Shukes *et al.* (2021) who found that there were only two sub-groups based on GPCR protein.

Based on the deduced amino acid sequences of RPO30 protein, phylogenetic analyses of the LSDA isolate showed that the Egyptian LSDA isolate is a part of a cluster and is closely related to other LSDV sequences from Sudan, Kenya, Mongolia, Russia and India. For the RPO30 protein, the amino acid sequence homology between the LSDA isolate and field strains from other nations was between 98.73%-100%, with the Sudan strains having the highest homology. The RPO30 protein multiple sequence alignments revealed amino acid sequence substitutions at F 183 S, M 60 I, L 84 S, G 158 E and W 159 C.

Peptide vaccines based on immunoinformatics overcome conventional vaccine side effects. Peptide vaccines can target rapidly mutating pathogens, can stimulate an effective immune response and require less time and cost to produce. The process that has come to be known as "reverse vaccinology", "vaccinomics", "immunome-derived vaccine" (IDV) design," or "genome-derived vaccine design" has been fueled by the availability of immunomemining tools Recognition of antigens occurs through the presentation of B cell and T cell epitopes that are derived from the protein sequence, in the appropriate immunological milieu. This vaccine concept is based on the identification of a minimal set of antigens that induces a competent immune response to a pathogen as mentioned by Marshall (2004). To combat the rapidly increasing and insatiable global burden of diseases, it is essential to develop a revolutionary vaccine (Fauci, 2006). The development of immunology knowledge and biotechnology in recent decades has accelerated the development of innovative methods for rational vaccine creation (Chaudhury *et al.*, 2020). By specifically stimulating antigen-specific B and T-cells, peptide-based vaccinations are intended to induce immunity against certain diseases (Purcell, 2007). Different peptide-based vaccines could be created using databases and powerful bioinformatics methods, where the peptides act as ligands and suggest interesting peptides for vaccine development (Usmani *et al.*, 2018).

The purpose of the current study was to use artificial intelligence to predict the immunogenic landscape of circulating lumpy skin disease in the Egyptian dairy cattle sector, which will lead to universal blueprints for multiepitope LSD vaccine designs. The study proposed a variety of peptides that can be recognized by B and T cells. Using the BCPreds, ABCpred, and SVMTriP Linear B epitopes prediction tools, it is predicted Linear B cell epitopes in this study. The three B-cell prediction tools detected 53 epitopes. The antigenicity, allergenicity and toxicity tests were successful for 12 promising and top Linear B epitopes. These peptides can effectively elicit an antibody response.

Using artificial neural networks, NetMHCpan 4.0, RANKPEP and IEDB MHC-I binding prediction tools, the LSDV GPCR, RPO30, P32 and EEV glycoproteins were further examined for MHC I and II binding epitopes. It was anticipated that 47 peptides would interact with various MHC class I alleles.

Seventeen of them (TLSFEMYK, TLSAYVIRL, LKIKKISVY, SLSFEMYKL, TLSDLIFVL, MIIPLTILL, NIFGMIIPL, VQFQQIKIM, TIACHLHVL, TLYSTIFFL, TLYSTIFFL, DMFLLNLTL, NVLDKKYNL, KKNFKPPKF, AQKFRVKLL, YKKKSSISF and KKSSISFSY) were generally encouraging and could bind to the largest number of MHC II alleles and passed the antigenicity and allergenicity and toxicity tests.

With a percentile rank less than or equal to 0.5, 49 predicted epitopes interacted with MHC-II alleles. Thirteen of them (FKKKGKNQK, FRFLISLKK, YSKNIYEIR, KYLFVNILF, KYFIFHVKI, KLMHKNNSE, FSFNIVQSR, YRLPKTKLK, YCYIFCVII MKLVAKFQM, YKYVKEKSK, SYSDNTTPT and WWFGLSQLL) were generally encouraging and could tie to the largest number of MHC-II alleles and passed the antigenicity and allergenicity and toxicity tests.

In this study, several B and T cell epitopes was found and could be used as antigenic targets in the creation of LSDV vaccines. However, to confirm these findings in the future, *in vivo* and *in vitro* studies will be required.

Conclusions and Recommendations

For epidemiological studies and the creation of new, effective LSDV vaccines, direct sequencing of PCR amplicons and comparative genetic analyses were helpful. One of the most effective public health strategies for reducing disease burden is vaccination. Because the vaccine targets the most important antigenic components of the pathogen, peptide vaccines have the potential to be safer and more effective than conventional vaccines. The predication of various peptides of LSDV GPCR, RPO30, P32 and EEV glycoproteins can be effectively protected cattle against LSDV, as demonstrated in this study. The antigenicity, allergenicity and toxicity tests were acceptable for 12 promising and top Linear B epitopes. An effective antibody response can be induced by these peptides. Thirteen peptides for MHC-II were chosen as the best targets for the vaccine. Seventeen MHC-I epitopes were the most promising because there ability to bind to a large number of MHC-I alleles and passed the antigenicity, allergenicity and toxicity tests. In order to confirm these findings in the future, in vivo and in vitro studies will be required.

Author's Contribution

All authors participated in the concept development, study execution, data analysis and interpretation processes. The first draught of the manuscript was written by all contributors. All authors had full access to all the study's data, accepted responsibility for the validity of the data and the accuracy of the analysis and gave their final approval before publication.

Ethical approval

All animal handling procedures, as well as sample collection and disposal were performed according to the pointers and recommendations of the European Communities Council Directive 1986 (86/609/EEC).

Conflict of interest

The authors have declared no conflict of interest.

References

Agianniotaki, E.I., Mathijs, E., Vandenbuss-che, F., Tasioudi, K.E., Haegeman, A., Iliadou, P., Chaintoutis, S.C., Dovas, C.I., Van Borm, S., Chondrokouki, E.D., and De Clercq, K., 2017. Complete genome sequence of the lumpy skin disease virus isolated from the first reported case in Greece in 2015. Genome Announcements, 5: e00550-17. https://doi.org/10.1128/genomeA.00550-17

Amin, A., El-Nahas, E., and El-Mashed, A., 2015. Pathological and virological studies on an outbreak of lumpy skin disease among cattle in Kalubia Governorate-Egypt. J. Adv. Vet. Res., 5(4): 165–175.

Awadin, W., Hussein, H., Elseady, Y., Babiuk, S., and Furuoka, H., 2011. Detection of lumpy skin disease virus antigen and genomic DNA in formalin-fixed paraffin-embedded tissues from an Egyptian outbreak in 2006. Transbound. Emerg. Dis., 58(5): 451–457. https://doi.org/10.1111/j.1865-1682.2011.01238.x

CFSPH, 2008. Center for food security and public health, Iowa State University. Lumpy Skin Disease. Accessed on July 17, 2017.

Chaudhury, S., Duncan, E.H., and Atre, T., 2020. Combining immunoprofiling with machine learning to assess the effects of adjuvant formulation on human vaccine-induced immunity. Hum. Vaccin. Immunother., 16(2): 400–411. https://doi.org/10.1080/21645515.2

019.1654807

Chibssa, T.R., Sombo, M., Lichoti, J.K., Adam, T.I.B., Liu, Y., Abd Elraouf, Y., Grabherr, R., Settypalli, T.B.K., Berguido, F.J., Loitsch, A., Sahle, M., Cattoli, G., Diallo, A., and Lamien, C.E., 2021. Molecular analysis of east African lumpy skin disease viruses reveals a mixed isolate with features of both vaccine and field isolates. Microorganisma, 9: 1142. https://doi.org/10.3390/microorganisms9061142

Davies FG (1991). Lumpy skin disease, an African capripox virus disease of cattle. Br. Vet. J., 147(6): 489–503. https://doi.org/10.1016/0007-1935(91)90019-J

Elhaig, M.M., Selim, A. and Mahmoud, M., 2017. Lumpy skin disease in cattle: Frequency of occurrence in a dairy farm and a preliminary assessment of its possible impact on Egyptian buffaloes. Onderstepoort J. Vet. Res., 84(1): e1–e6. https://doi.org/10.4102/ojvr.v84i1.1393

El-Tholoth, M., and El-Kenawy, A., 2016. G-protein-coupled chemokine receptor gene in lumpy skin disease virus isolates from cattle and water buffalo (*Bubalus bubalis*) in Egypt. Transbound. Emerg. Dis., 63: 288-295. https://doi.org/10.1111/tbed.12344

Fauci, A.S., 2006. Emerging and re-emerging infectious diseases: Influenza as a prototype of the host-pathogen balancing act. Cell, 124(4): 665–670. https://doi.org/10.1016/j.cell.2006.02.010

Gelaye, E., Belay, A., Ayelet, G., Jenberie, S., Yami, M., Loitsch, A., Tuppurainen, E., Grabherr, R., Diallo, A., and Lamien, C.E., 2015. Capripox disease in Ethiopia: genetic differences between field isolates and vaccine strain, and implications for vaccination failure. Antiviral Res., 119: 28-35. https://doi.org/10.1016/j.antiviral.2015.04.008

Ireland, D.C. and Binepal, Y.S., 1998. Improved detection of capripox virus in biopsy samples by PCR. J. Virol. Methods, 74(1): 1-7. https://doi.org/10.1016/S0166-0934(98)00035-4

Le Goff, C., Lamien, C.E., Fakhfafh, E., Chadeyras, A., Abu Adulugbad, E., Libeau, G., Tuppurainen, E., Wallace, D., Adam, T., Silber, R., Gulyaz, V., Madani, H., Caufour, P., Hamammi, S., Diallo, A., and Albina, E., 2009. Capripoxvirus G-protein-coupled chemokine receptor, a host-range gene suitable for virus-animal origin discrimination. J. Gen. Virol., 90 : 67–77. https://doi.org/10.1099/vir.0.010686-0

Lefèvre, P.C., and Gourreau, J.M., 2010. Lumpy skin disease. In: Lefèvre PC, Blancou J, Chermette R, Uilenberg G (Eds.) Infectious and Parasitic diseases of Livestock. OIE -407. https://doi.org/10.1079/9782743008727.0000

Lu, G., Xie, J., Luo, J., Shao, R., Jia, K., and Li, S., 2020. Lumpy skin disease outbreaks in china, since 3 August 2019. Transbound. Emerg. Dis., https://doi.org/10.1111/tbed.13898

Manic, M., Stojiljkovic, M., Petrovic, M., Nisavic, J., Bacic, D., *et al.*, 2019. Epizootic features and control measures for lumpy skin disease in south-east Serbia in 2016. Transbound. Emerg. Dis., 66: 2087-2099. https://doi.org/10.1111/tbed.13261

Marshall, S.J., 2004. Developing countries face double burden of disease. Bull. World Health Organ., 82: 556.

OIE, 2010. Lumpy skin disease. In: Manual of diagnostic tests and vaccine terrestrial animals. OIE, Paris, pp. 1–13.

OIE, 2017. World Organization for Animal Health. Lumpy Skin Disease. Terrestrial Animal Health Code.

Purcell, A.W., McCluskey, J., and Rossjohn, J., 2007. More than one reason to rethink the use of peptides in vaccine design. Nat. Rev. Drug Discovery, 6(5): 404–414. https://doi.org/10.1038/nrd2224

Sameea, P., Mardani, K., Dalir-Naghadeh, D., Jalilzadeh and Amin, G., 2016. Epidemiological study of lumpy skin disease outbreaks in northwestern Iran. Transbound Emerg Dis, 64: 1782-1789. https://doi.org/10.1111/tbed.12565

Shukes, C.B., Chowdhury, M.G.A., Settypalli, T.B.K., Cattoli, G., Lamien, C.E., Fakir, M.A.U., Akter, S., Osmani, M.G., Talukdar, F., Begum, N., Khan, I.A., Rashid, M.B. and Sadekuzzaman, M., 2021. Molecular characterization of lumpy skin disease virus (LSDV) emerged in Bangladesh reveals unique genetic features compared to contemporary field strains. BMC Vet. Res., 17: 61. https://doi.org/10.1186/s12917-021-02751-x

Sohier, C., Haegeman, A., Mostin, L., De Leeuw, I., Van Campe, W., De Vleeschauwer, A., Tuppurainen, E.S.M., Berg, T.V.D., De Regge, N. and De Clercq, K., 2019. Experimental evidence of mechanical lumpy skin disease virus

transmission by *Stomoxys calcitrans* biting flies and *Haematopota* spp. horseflies. Sci. Rep., 9: 20076. https://doi.org/10.1038/s41598-019-56605-6

Sprygin, A., Artyuchova, E., Babin, Y., Prutnikov, P., Kostrova, E., Byadovskaya, O., and Kononov, A., 2018a. Epidemiological characterization of lumpy skin disease outbreaks in Russia in 2016. Transbound. Emerg. Dis., 65: 1514-1521. https://doi.org/10.1111/tbed.12889

Sprygin, A., Babin, Y., Pestova, Y., Kononova, S., Wallace, D., Van Schalkwyk, A., Byadovskaya, O., Diev, V., Lozovoy, D., and Kononov, A., 2018b. Analysis and insights into recombination signals in lumpy skin disease virus recovered in the field. PLoS One, 13: e0207480. https://doi.org/10.1371/journal.pone.0207480

Sudhakar, B.S., Mishra, N., Kalaiyarasu, S., Jhade, K.S., Hemadri, D., *et al.*, 2020. Lumpy skin disease (LSD) outbreaks in cattle in Odisha state, India in August 2019: Epidemiological features and molecular studies. Transbound. Emerg. Dis., 67: 2408-2422. https://doi.org/10.1111/tbed.13579

Tageldin, M.H., Wallace, D.B., Gertdes, G.H., Putterill, J.F., Greyling, R.R., *et al.*, 2014. Lumpy skin disease of cattle: an emerging problem in the Sultanate of Oman. Trop. Anim. Health Prod., 46: 241-246. https://doi.org/10.1007/s11250-013-0483-3

Tasioudi, K.E., Antoniou, S.E., Iliadou, P., Sachpatzidis, A., Plevraki, E., Agianniotaki, E.I., Fouki, C., Mangana-Vougiouka, O., Chondrokouki, E., and Dile, C., 2016. Emergence of lumpy skin disease in Greece, 2015. Transbound. Emerg. Dis., 63: 260–265. https://doi.org/10.1111/tbed.12497

Tulman, E.R., Afonso, C.L., Lu, Z., Zsak, L., Kutish, G.F., and Rock, D.L., 2001. Genome of lumpy skin disease virus. J. Virol., 75: 7122–7130. https://doi.org/10.1128/JVI.75.15.7122-7130.2001

Usmani, S.S., Kumar, R., Bhalla, S., Kumar, V., and Raghava, G.P.S., 2018. In silico tools and databases for designing peptide-based vaccine and drugs. Ther. Proteins Peptides, 112: 221–263. https://doi.org/10.1016/bs.apcsb.2018.01.006

Van Rooyen, P.J., Munz, E.K. and Weiss, K.E., 1969. The optimal conditions for the multipliction of neethling type lumpy skin disease virus in embryonated eggs. J. Vet. Res., 36: 165–174.

Wassie, M., Klaas, F., Getachew, G., Menbere, K., Dereje, S., and Mart, C.M.J., 2018. Seroprevalence and risk factors of lumpy skin disease in Ethiopia. Prev. Vet. Med., 160(15): 99-104. https://doi.org/10.1016/j.prevetmed.2018.09.029